TFEB-Mediated Lysosomal Restoration Alleviates High Glucose-Induced Cataracts Via Attenuating Oxidative Stress

Yan Sun, Xiaoran Wang, Baoxin Chen, Mi Huang, Pengjuan Ma, Lang Xiong, Jingqi Huang, Jieping Chen, Shan Huang, and Yizhi Liu

State Key Laboratory of Ophthalmology, Zhongshan Ophthalmic Center, Sun Yat-Sen University, Guangzhou, China

Correspondence: Shan Huang, Zhongshan Ophthalmic Centre, Sun Yat-Sen University, No. 7 Jinsui Road, Guangzhou 510060, China; huangsh29@mail.sysu.edu.cn.

Received: November 16, 2021
Accepted: June 8, 2022
Published: June 27, 2022

Citation: Sun Y, Wang X, Chen B, et al. TFEB-mediated lysosomal restoration alleviates high glucose-induced cataracts via attenuating oxidative stress. *Invest Ophthalmol Vis Sci.* 2022;63(6):26. https://doi.org/10.1167/iovs.63.6.26

Purpose. Diabetic cataract (DC) is a visual disorder arising from diabetes mellitus (DM). Autophagy, a prosurvival intracellular process through lysosomal fusion and degradation, has been implicated in multiple diabetic complications. Herein, we performed in vivo and in vitro assays to explore the specific roles of the autophagy-lysosome pathway in DC.

Methods. Streptozotocin-induced DM and incubation in high glucose (HG) led to rat lens opacification. Protein Simple Wes, Western blot, and immunoassay were utilized to investigate autophagic changes in lens epithelial cells (LECs) and lens fiber cells (LFCs). RNA-sequencing (RNA-seq) was performed to explore genetic changes in the lenses of diabetic rats. Moreover, autophagy-lysosomal functions were examined using lysotracker, Western blot, and immunofluorescence analyses in HG-cultured primary rabbit LECs.

Results. First, DM and HG culture led to fibrotic LECs, swelling LFCs, and eventually cataracts. Further analysis showed aberrant autophagic degradation in LECs and LFCs during cataract formation. RNA-seq data revealed that the differentially expressed genes (DEGs) were enriched in the lysosome pathway. In primary LECs, HG treatment resulted in decreased transcription factor EB (TFEB) and cathepsin B (CTSB) activity, and increased lysosomal size and pH values. Moreover, TFEB-mediated dysfunctional lysosomes resulted from excessive oxidative stress in LECs under HG conditions. Furthermore, TFEB activation by curcumin analog C1 alleviated HG-induced cataracts through enhancing lysosome biogenesis and activating protective autophagy, thereby attenuating HG-mediated oxidative damage.

Conclusions. In summary, we first identified that ROS-TFEB-dependent lysosomal dysfunction contributed to autophagy blockage in HG-induced cataracts. Additionally, TFEB-mediated lysosomal restoration might be a promising therapeutic method for preventing and treating DC through mitigating oxidative stress.

Keywords: diabetic cataract (DC), lens, autophagy, lysosome, transcription factor EB (TFEB)

Diabetes mellitus (DM) is a global metabolic disease and contributes to multiple ocular disorders. Diabetic cataract (DC), which develops over time, is the most common vision-threatening complication of DM.[1] The incidence of cataracts in patients with diabetes is five times higher than in those without diabetes.[2] Although cataract surgery is common and effective in treating DC, the high frequency of surgery-related side effects, such as impaired wound healing and secondary glaucoma, is associated with poor clinical outcomes.[3] Hence, it is necessary to explore the pathogenesis and provide a pharmacologic treatment paradigm for preventing the occurrence and progression of hyperglycemia complicated with cataracts. The lens is composed of a monolayer of cuboidal lens epithelial cells (LECs) and highly elongated and aligned lens fiber cells (LFCs),[4] dysfunctions of either of which can lead to cataracts.[5] Under high glucose (HG) conditions, the overactivation of aldose reductase (AR) converts glucose into sorbitol, leading to hyperosmotic stress and oxidative damage in the lens.[6] Excessive generation of reactive oxygen species (ROS) can induce epithelial-mesenchymal transition (EMT) and apoptosis of LECs, further leading to dysfunction of LFCs,[7,8] which is also a critical mechanism of other diabetic complications.[9] Although drugs for AR inhibitors and antioxidants have been developed in the past decades, there is still a lack of effective drugs for DC clinically.[10–12] Therefore, it is necessary to continue exploring the molecular mechanisms of DC for investigating more effective therapeutic strategies to prevent or delay the progression of DC.

To further investigate the pathogenesis of DC, RNA sequencing (RNA-seq) analysis was performed to explore molecular changes in streptozotocin (STZ)-induced DC. In addition to upregulation of oxidative damage and advanced glycation end products (AGEs) related pathways, lysosomal pathway genes were downregulated in the lenses of diabetic rats, suggesting that lysosomal dysfunction might

be involved in the pathogenesis of DC occurrence. Increasing evidence shows that autophagy participates in the pathogenesis of diabetes by regulating insulin signaling and lipid metabolism.[13] Autophagy is a lysosome-dependent degradation pathway, which maintains cellular homeostasis and defends against external stresses.[14] Pathogenic factors, such as nutrient deficiency, hypoxia, and inflammation, stimulate adaptive or destructive autophagy, thus protecting tissues or accelerating tissue damage.[15] In the autophagy-lysosomal process, abnormally folded proteins and damaged organelles are recognized and engulfed by autophagosomes and then degraded by lysosomal enzymes.[14] If these macromolecules cannot be digested by lysosomes, overloaded autophagic substrates in cells ultimately lead to tissue and organ malfunction. Recent studies show that impairment of the autophagy-lysosomal pathway promotes the progression of hyperglycemia-related complications, such as diabetic nephropathy and diabetic retinopathy.[16,17] However, the functional impact of autophagy in cataractogenesis under diabetic conditions remains relatively unexplored.

The autophagy-lysosomal pathway has been revealed to participate in lens development. During embryonic lens formation, the differentiation from lens epithelial to fiber relies on autophagy to degrade the nucleus and organelles, and eventually forms the organelle-free zone (OFZ).[18] Autophagy gene mutations of FYCO1 caused congenital cataracts by suppressing lysosome trafficking and phagosome maturation.[19,20] Besides, deficiency of ATG5 resulted in age-related cortical cataracts due to the accumulation of insoluble oxidized proteins in fiber cells.[21] Researchers have preliminarily observed that autophagy was impaired in LECs upon exposure to HG conditions.[22] Autophagy is a dynamic process that includes the following steps: autophagosome formation, autophagosome-lysosome fusion, and cargoes degradation, and failure of any process will result in blockage of autophagy. However, it remains unknown at which stage autophagy dysfunction might occur in the lens under diabetic conditions.[22]

Here, we explored the biological function and molecular effects and mechanisms of the autophagy-lysosomal pathway in HG-induced cataracts. The results showed that lysosomal dysfunction induced by HG resulted in autophagic flux blockage in the lens cells during DC occurrence. Meanwhile, we identified that HG-induced lysosomal deficiency in LECs was due to defects of a key transcription factor responsible for lysosomal biogenesis, transcription factor EB (TFEB), in a ROS-dependent manner. Furthermore, TFEB activation by curcumin analog C1 (C1) relieved the development of HG-induced cataracts by enhancing lysosomal degradation, promoting autophagic flux, and finally attenuating oxidative stress. In summary, this study reveals a lysosomal degradation as a novel mechanism for the pathogenesis of DC, modulation of which might provide a therapeutic option for the prevention and treatment of DC.

Materials and Methods

Establishment of Diabetic Animal Model

All animal experiments were performed following the ARVO Statement for the Use of Animals in Ophthalmic and Vision Research under ethical approval of the Animal Ethics of Sun Yat-Sen University. Six-week-old Sprague-Dawley (SD) rats in the DM group were injected intraperitoneally with 60 mg/kg STZ dissolved in citrate buffer. The standard of our diabetic model was defined as the blood glucose level higher than 16.7 mmol/L at 72 hours after STZ injection. After the anterior segments of the eyes were photographed using a slit lamp (the third month), the lenses were micro-dissected from other ocular tissues and photographed through a stereomicroscope. The severity of cataracts was scored based on previous studies on diabetic rats.[23]

RNA-Sequencing

The transcriptome sequencing analysis of whole lenses in the control group ($n = 4$) and the DC group ($n = 8$) were performed by OE Biotech Co., Ltd. (Shanghai, China) with a higher sequence platform (Illumina). After quality control, the clean reads were aligned to the rat reference genome using Hisat2. The read counts of each gene were obtained from HTSeq-count, and the gene expression level was normalized by the fragments per KB million (FPKM) method. The significant threshold values for differentially expressed genes (DEGs) between the control and DC groups were defined as P value < 0.05 and fold change >2 or <0.5. Gene Ontology (GO) and Kyoto Encyclopedia of Genes and Genomes (KEGG) pathway enrichment analyses of the downregulated and upregulated DEGs were performed using R statistical software.

Immunohistochemistry and Immunofluorescence Assays

For hematoxylin and eosin (H&E) staining and immunohistochemistry, whole rat lenses in our study were fixed in 10% formalin and embedded in paraffin. In immunohistochemistry, the slides were blocked in phosphate-buffered saline (PBS) containing 0.3% Triton X-100 and 3% bovine serum albumin (BSA) for 30 minutes at room temperature (RT) and incubated with primary antibodies at 4°C overnight. After incubation with biotin-conjugated secondary antibodies, the visualization was performed with a DAB staining kit. In immunofluorescence, lenses were fixed in 4% paraformaldehyde (PFA) in PBS and embedded in OCT and cultured LECs were fixed at 4% PFA. After blocking in PBS containing 0.3% Triton X-100 and 3% BSA and incubation with primary antibodies, the cryosections were incubated with fluorescent secondary antibodies. DAPI counterstain was utilized for cell nuclei visualization. Finally, the images were taken by a Leica microscope (DM3000).

The primary antibodies used in immunohistochemistry and immunofluorescence assays were as follows: α-SMA (ab7817; Abcam), FN (ab137720; Abcam), Ki67 (AB9260; Millipore), DNASE 2B (NBP2-16199; Novus), P62 (ab56416; Abcam), TFEB (sc-166736; Santa Cruz), and LAMP1 (NB120-19294; Novus).

Ex Vivo Lens Culture and Treatment

Whole lenses were carefully isolated from the eyeballs of 5-week-old SD rats as previously described.[24] Then the lenses were transferred to 12-well plates and cultured in Dulbecco's Modified Eagle Medium (DMEM; 5.5 mM glucose) supplemented with 1% fetal bovine serum (FBS). Lenses that maintained transparency after 24 hour's culture were selected and randomly divided into the control normal glucose group (NG; 5.5 mM) and the high glucose (HG; 50 and 100 mM) groups. To study the effects of TFEB activation, we treated

lenses with curcumin analog C1 (C1; 5 µM; Selleck) or tetrahydrocurcumin (THC; 5 µM; Selleck) upon HG (50 mM) treatment. After incubation for 7 days, the lenses were observed and photographed by a stereomicroscope. Lens opacification was evaluated the same way as above.

Isolation, Culture, and Treatment of Primary LECs

We isolated and cultured primary LECs from the lenses of 2-month-old New Zealand White rabbits, as previously described.[25] To identify the effects of HG on autophagy in primary LECs, LECs were treated with HG medium at different concentrations. Pretreatment of N-acetylcysteine (NAC; 5 mM) in advance for 8 hours before HG (25 mM) treatment was used to inhibit HG-induced ROS production in LECs. To further study the TFEB activation mechanism, C1 (5 µM) or THC (5 µM) was added to the culture medium containing 25 mM glucose.

Transmission Electron Microscopy

After treatment, separated lens capsules and primary LECs were fixed in 2.5% glutaraldehyde. Then the tissues and cells were washed with PBS and post-fixed in 1% osmium (VIII) oxide for 1 hour. After dehydration in ethanol, the samples were embedded in epoxy resin. The ultrathin sections were captured by using a Tecnai G2 Spirit.

Automated Western Immunoblotting (Protein Simple Wes) and Western Blot Analysis

For protein expression analysis of lenses, we separated the anterior capsule with attached LECs from the fiber cell mass according to previous literature.[26] For extracting total proteins, the lens tissues and cells were lysed with radioimmunoprecipitation (RIPA) buffer containing phenylmethanesulfonyl fluoride (PMSF). Proteins in the cytoplasm and nuclei were separated by NE-PER Nuclear and Cytoplasmic Extraction Reagents (Thermo Scientific).

The Protein Simple Wes immunoassay performed the protein analyses of LECs of our diabetic model according to the instruction provided by the manufacturer (Protein Simple).[27] The Compass software (Protein Simple) was applied to present the Western immunoblots. Other proteins were separated by sodium dodecylsulphate-polyacrylamide gel electrophoresis (SDS-PAGE) gels and transferred to polyvinylidene difluoride (PVDF) membranes. After blocking and incubation with the primary antibodies, the membranes were incubated with HRP-conjugated secondary antibodies. Finally, the protein bands were detected and analyzed with a Bio-Rad Protein Assay.

The primary antibodies used in Western blot analysis were as follows: α-SMA (ab7817; Abcam), FN (ab137720; Abcam), LC3B (83506; Cell Signaling Technology, CST), P62/Sequestosome 1 (ab56416; Abcam), ATG7 (8558T; CST), ATG5 (12994; CST), LAMP1(NB120-19294; Novus), CTSB (31718; CST), TFEB (37785; CST), ZKSCAN3(223477; Abcam), phospho-mTOR (5536; CST), mTOR (2983; CST), DNASE 2B (NBP2-16199; Novus), β-Actin (3700; CST), α-Actinin (6487; CST), GAPDH (2118; CST), and Lamin B1 (13435; CST).

Lysotracker Assay

Lysotracker (Invitrogen) was used to label and track the acidification of lysosomes according to the manufacturer's guidelines. Cells were incubated with the Lysotracker probe-containing medium for 30 minutes. For quantification and assessment of lysosomes, images of the Lysotracker-stained LECs were captured by a microscope directly.

mCherry-EGFP-LC3 Plasmid Transduction

Primary LECs were transduced with mCherry-EGFP-LC3 plasmid by using Lipofectamine 3000 Reagent (Invitrogen) based on the manufacturer's instructions. After transduction for 24 hours, then transiently mCherry-EGFP-LC3-expressed LECs were cultured under different conditions for 48 hours. Yellow spots represented autophagosomes, and red spots represented autolysosomes. The number of autophagosomes and autolysosomes was quantified in five random fields under a fluorescence microscope.

Detection of ROS Using the DCFH-DA

We measured intracellular ROS production in LECs using the fluorescent probe DCFH-DA (Beyotime). After incubation in DCFH-DA (10 µM) for 20 minutes, the cells were observed by fluorescence microscopy to compare the ROS generation.

Quantitative Real-Time PCR

Total RNA of LECs was extracted using the Rneasy Mini Kit (Qiagen). PrimeScript RT Master Mix (Takara) was used for reverse transcription assay. We performed quantitative real-time PCR (qRT-PCR) reactions on a Step One Plus real-time PCR system (Applied Biosystems) using QuantiNovaTM SYBR Green PCR kit (Qiagen). The relative expression levels of mRNAs were calculated using the $2^{-\Delta\Delta Ct}$ method.

Cell Transfection

To knock down gene expression of TFEB, small interfering RNA (siRNA) of the negative control (siNC) and TFEB (siTFEB) were transfected into primary rabbit LECs using Lipofectamine 3000 agent. When LECs seeded into the 6-well plates were grown to 70% confluence, the transfection mixtures were premixed well for 15 minutes and then added into each well. After transfection for 24 hours, the successfully transfected cells were applied in subsequent experiments.

Statistics

The statistical significance was analyzed using GraphPad Prism software version 7.0. The results were compared using the Student's *t*-test between two groups and 1-way ANOVA among multiple groups, respectively. A P value less than 0.05 was considered statistically significant.

Results

STZ-Induced Diabetic Cataracts Exhibited Impaired Autophagic Flux

Changes in blood glucose for 3 months are presented in Supplementary Figure S1. All rats in the DM group developed cataracts with varying degrees, whereas all control lenses still maintained transparency (Fig. 1A). The most frequently observed cataracts in the DM group were cortical opacities, ranging from score 1 to 5 (Fig. 1A). As shown in Figures 1C, 1D, an apparent upregulation of α-SMA, FN, as well as proliferative marker Ki67 in LECs in the DM group

Investigative Ophthalmology & Visual Science

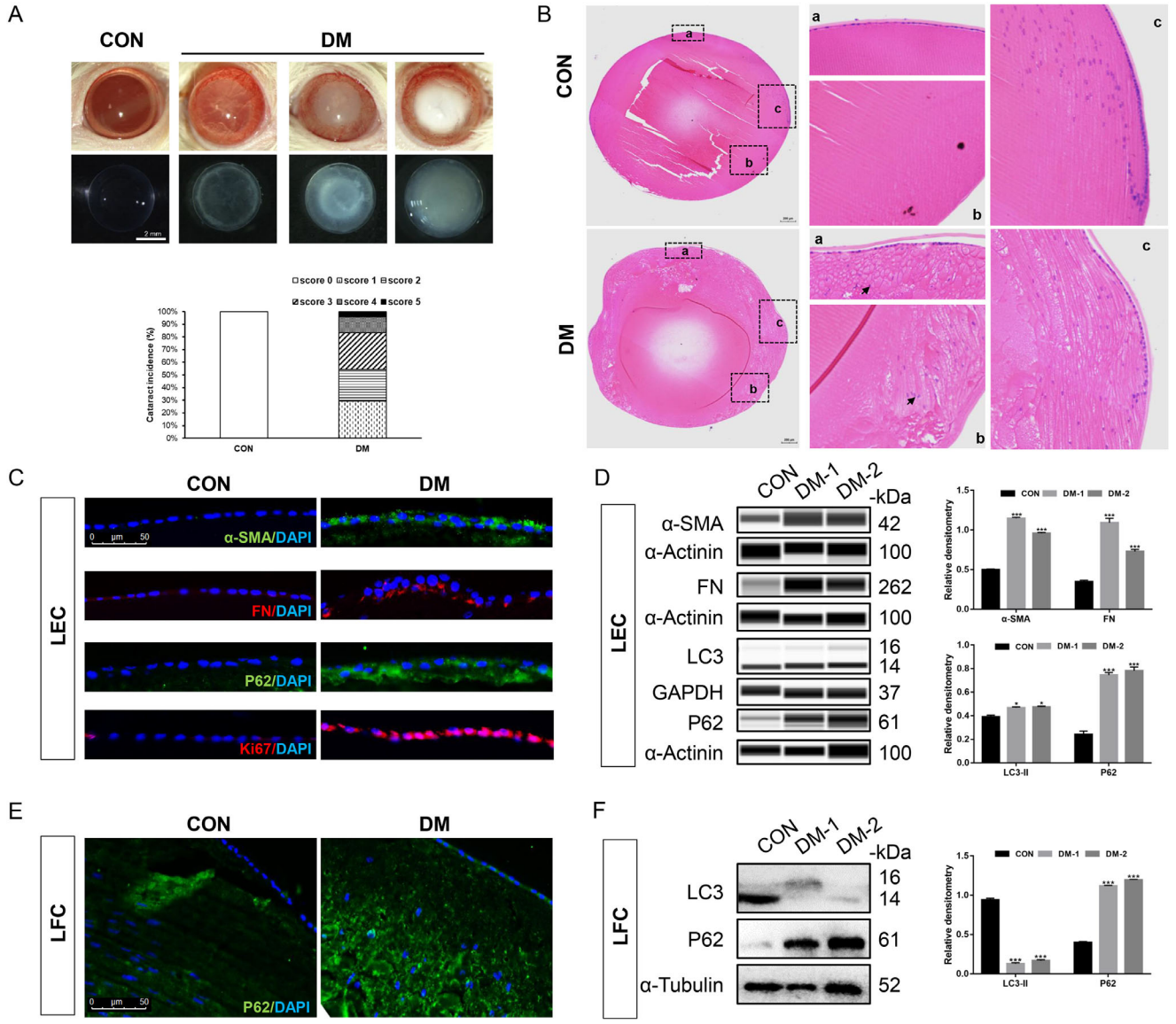

Figure 1. STZ-induced diabetic cataracts exhibited impaired autophagic flux. Rats were injected with STZ for 3 days to induce diabetes, whereas rats in the control group were injected with citrate buffer only. Then, these rats were raised under normal conditions for three months, and their blood glucose levels were monitored every 7 days. (**A**) Representative images of the anterior segment of the eye using slit-lamp examination and extracted lenses in two groups and the percentage distribution of cataract scores. Cataract score: no cataract (0), peripheral vesicles and opacities (1), central opacities (2), diffuse central opacities (3), mature cataract (4), and hypermature cataract (5). (**B**) H&E staining of rat lenses at 12 weeks (a: anterior central zone; b: posterior cortical zone; and c: equatorial zone). There were prominent lens fiber swelling and aberrant nuclei (*arrows*) in the DM group, compared to the control group. (**C**) Immunofluorescence staining of α-SMA, FN, Ki67, and P62 in the anterior subcapsular LECs. (**D**) Automated western immunoblotting determined the changes of the mesenchymal markers (α-SMA and FN) and autophagy markers (LC3-I/II and P62) in LECs. (**E**) Immunofluorescence staining of P62 in LFCs located along the equatorial zone. (**F**) Densitometry quantification of LC3-II and P62 in LFCs by Western blot analysis. Relative protein levels of total proteins were standardized to the expression of GAPDH, α-Tubulin, or α-Actinin. All the data were shown as mean ± standard deviation. $^{*}P < 0.05$, $^{**}P < 0.01$, and $^{***}P < 0.001$.

indicated EMT activation upon STZ-induced diabetes. H&E staining showed that cortical fiber cells exhibited swelling and vacuoles in the DM group (see Fig. 1B). In terms of autophagy, we monitored the autophagic flux by assessing the expression levels of LC3-II (the autophagosome marker) and P62 (the autophagic substrate). Compared to the control group, the level of LC3-II was elevated in LECs and declined in LFCs in the DM group (Figs. 1C–F). Notably, diabetes contributed to a prominent accumulation of P62 in both LECs and LFCs, suggesting inhibited autophagic flux. Overall, these results suggested that autophagy defects during STZ-induced diabetic cataracts progression might lead to abnormal LECs and LFCs.

HG Led to Autophagy Blockage in Ex Vivo Lens Organ Culture

In isolated lens organ culture for 7 days, all lenses cultured in HG medium (50 and 100 mM) developed cortical cataracts ranging from score 1 to 3, whereas the control lenses remained clear (Fig. 2A). Additionally, HG-cultured lenses

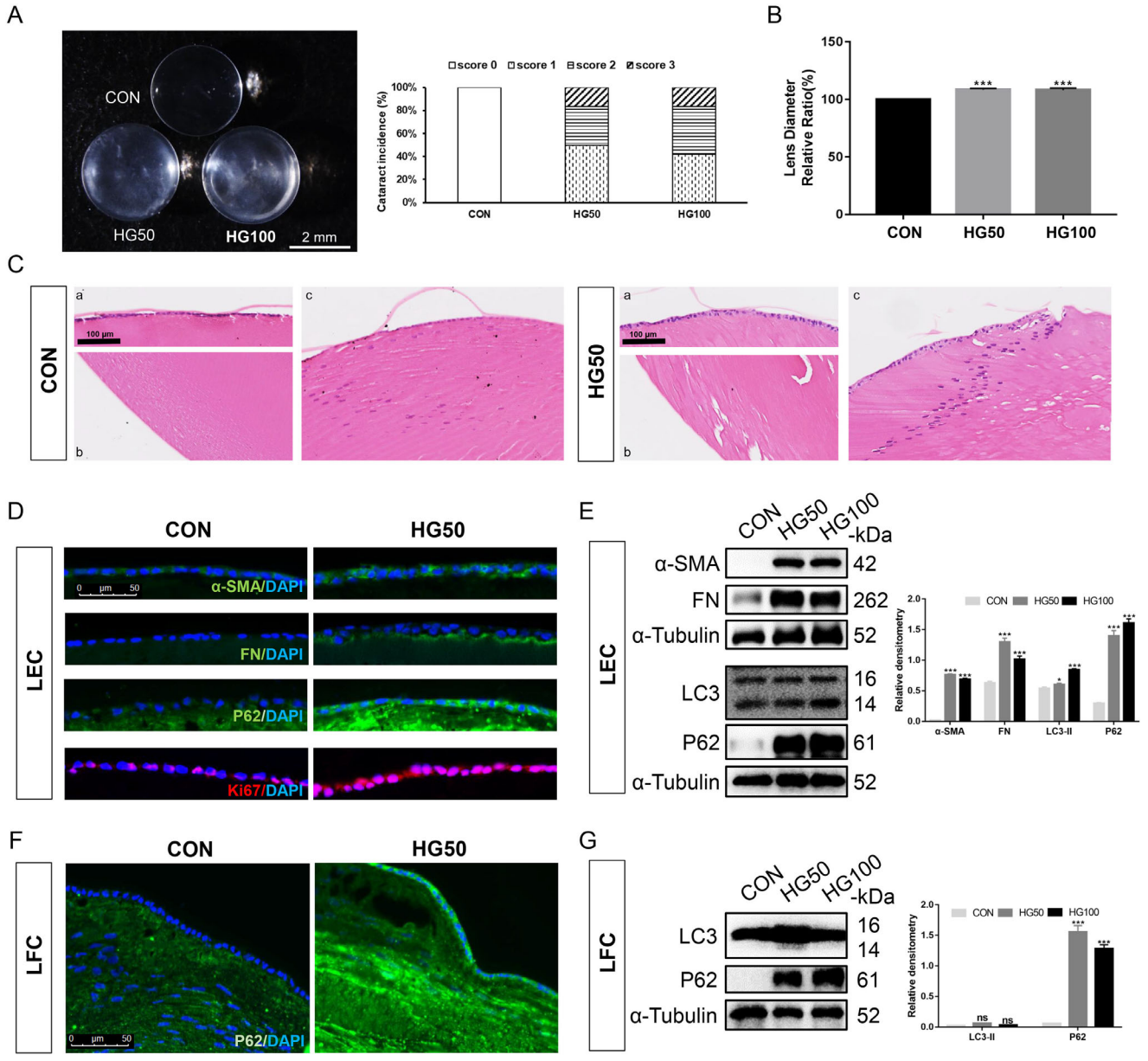

Figure 2. HG led to autophagy blockage in *ex vivo* lens organ culture. The rat lenses were cultured in HG medium (50 and 100 mM) for 7 days. (**A**) Representative images of cultured rat lenses and the percentage distribution of cataract scores in control, HG50, and HG100 groups. (**B**) Lens diameter ratio was relative to the control group. (**C**) H&E staining of cultured lenses in the control and HG (50 mM) groups (a: anterior central zone; b: posterior cortical zone; and c: equatorial zone). (**D**) Immunofluorescence staining of α-SMA, FN, Ki67, and P62 in anterior subcapsular LECs. (**E**) Densitometry quantification of α-SMA, FN, LC3-I/II, and P62 in LECs by Western blot analysis. (**F**) Immunofluorescence staining of P62 in LFCs located along the equatorial zone. (**G**) Densitometry quantification of LC3-II and P62 in LFCs by Western blot analysis. Relative protein levels of total proteins were standardized to the expression of α-Tubulin. All the data were shown as mean ± standard deviation. $^{*}P < 0.05$, $^{**}P < 0.01$, and $^{***}P < 0.001$.

appeared slightly larger in diameter (Fig. 2B) and remarkable swelling in lens fibers (Fig. 2C) than NG-cultured lenses. In concert with our findings above, HG significantly enhanced the EMT process and proliferative capacity in LECs (Figs. 2D, 2E). Moreover, the expression level of LC3-II was significantly upregulated in LECs but without differences in LFCs, and P62 exerted an upregulation trend in LECs and LFCs (see Figs. 2D–G). Although the changes of LC3-II were found to be discordant between LECs and LFCs, a noticeable accumulation of P62 still indicated that the autophagic flux was inhibited under HG conditions. These results confirmed that it was HG that caused intracellular autophagy arrest and cellular abnormalities in both LECs and LFCs in diabetes.

STZ-Induced Diabetes Led to the Aberrant Expression of Lysosome-Related Pathways in the Lens

To investigate the molecular mechanism of DC, we explored the genomewide changes characterizing DC formation in

Investigative Ophthalmology & Visual Science

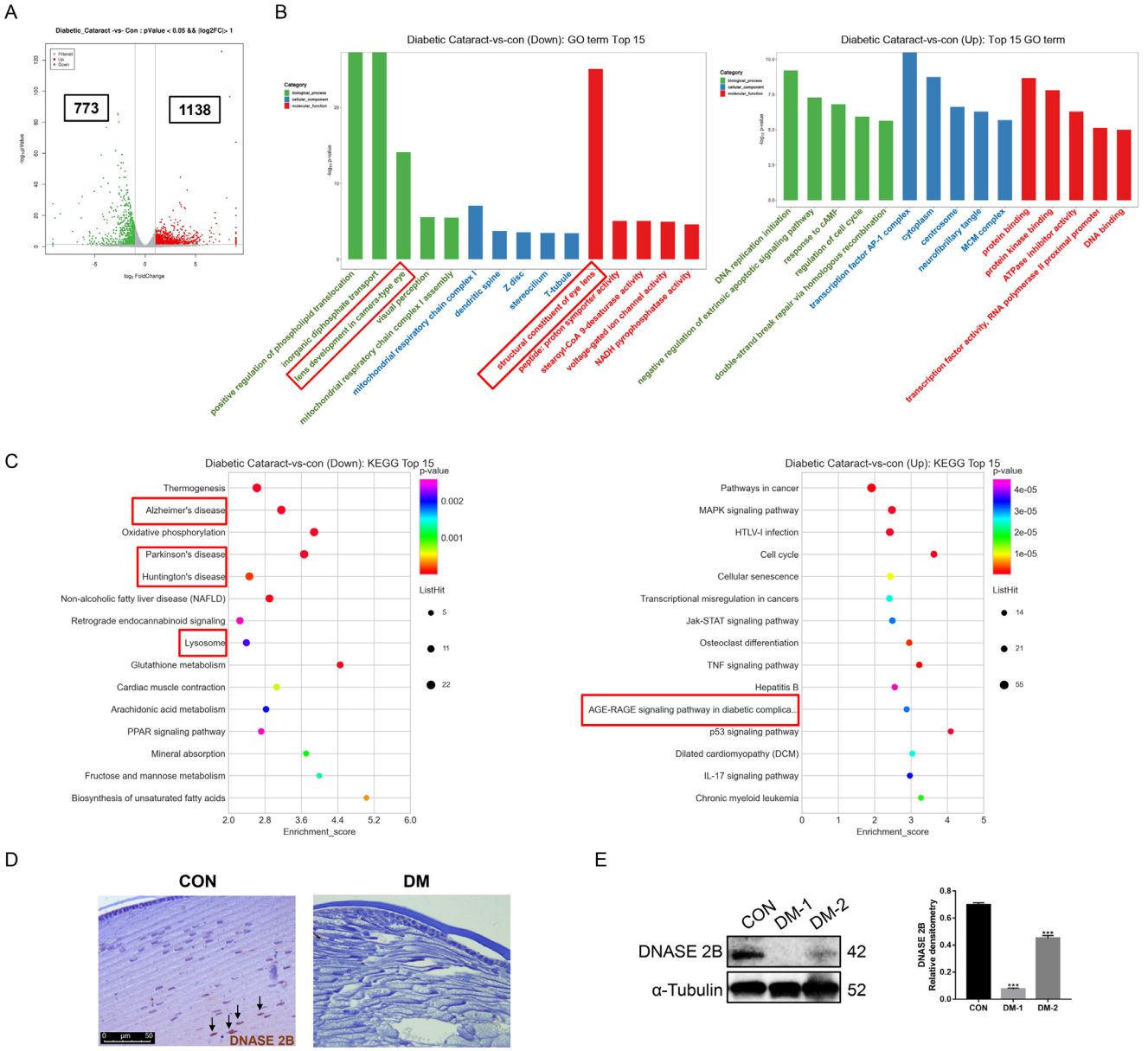

Figure 3. Comparative transcriptome analysis of lenses between the control group and DM group. The lenses in the control group ($n = 4$) and the DM group ($n = 8$) were compared to identify DEGs using RNA-seq analysis. (**A**) Volcano plot. (**B**) GO enrichment analysis and (**C**) KEGG pathway enrichment analysis of the downregulated and upregulated DEGs, respectively. (**D**) Immunohistochemical staining of DNASE 2B (*arrows*) in lens fibers located along the equatorial zone and (**E**) densitometry quantification of DNASE 2B in LFCs by Western blot analysis. Relative protein levels of total proteins were standardized to the expression of α-Tubulin. All the data were shown as mean ± standard deviation. *$P < 0.05$, **$P < 0.01$, and ***$P < 0.001$.

vivo using RNA-seq technology. Supplementary Figure S2 exhibited the principal component analysis (PCA). A total of 1138 upregulated and 773 downregulated genes were screened between the DC and control groups (Fig. 3A). The GO analysis demonstrated that the downregulated DEGs were predominantly involved in lens development and structural constituent of eye lens (Fig. 3B; Supplementary Table S1). Interestingly, the KEGG enrichment analysis showed that the downregulated DEGs happened to be significantly enriched in Huntington's disease, Parkinson's disease, Alzheimer's disease, and the lysosome pathway (Fig. 3C). It is noteworthy that these neurodegenerative diseases all belong to lysosomal storage diseases (LSDs).[28] Among the differentially expressed lysosomal genes (Supplementary Table S2), we detected the expression of DNase II-like acid nuclease DNase IIβ (DNASE 2B) for verification. DNASE 2B is uniquely localized in the nucleus of lens cortical fibers, participating in nuclear DNA degradation during LECs differentiation into LFCs.[29] The expression of DNASE 2B in the diabetic LFCs was significantly lower than that in the normal LFCs (Figs. 3D, 3E). Moreover, we found that nuclei aberrantly existed in the anterior and posterior subcapsular cortex (see Fig. 1B), which should have been degraded to form the OFZ. Taken together, the bioin-

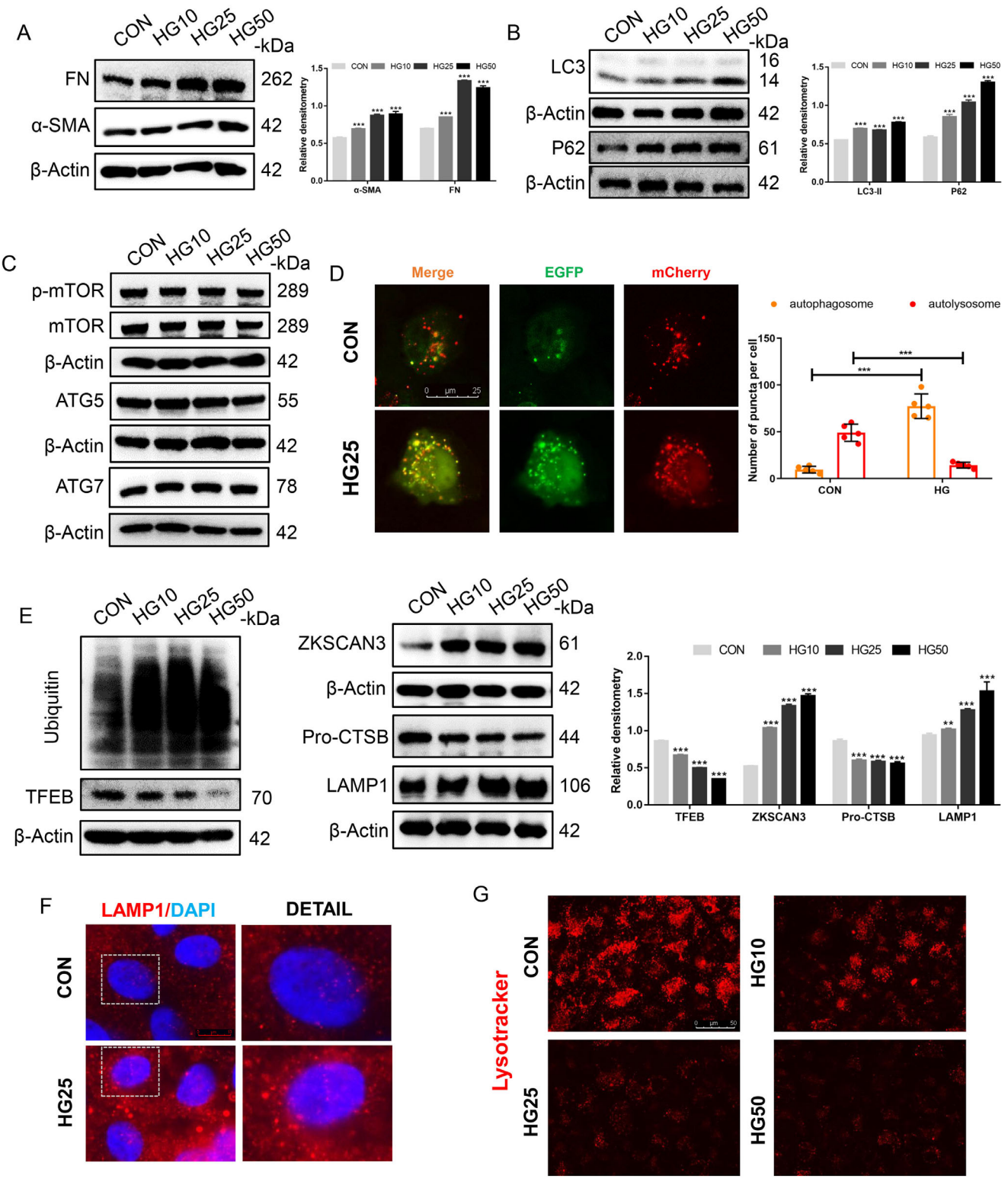

Figure 4. HG-induced autophagy blockage was due to TFEB-mediated lysosomal dysfunction in LECs. LECs were treated with various concentrations of glucose (5, 10, 25, and 50 mM) for 3 days. (**A–C**) Western blot analysis showed the effects of glucose on the changes of mesenchymal markers (α-SMA and FN) and autophagic markers (LC3-I/II, P62, p-mTOR, mTOR, ATG7, and ATG5). (**D**) Representative fluorescence images of mCherry-EGFP-LC3 puncta within LECs and quantification. Yellow puncta: autophagosomes, red-only puncta: autolysosomes. (**E**) Western blot analysis showed the expression of lysosome-associated proteins (ubiquitin, TFEB, ZKSCAN3, Pro-CTSB, and LAMP1) upon HG stimulation. (**F**) Immunofluorescence staining of LAMP1 puncta within LECs. (**G**) Lysotracker assay showed reduced lysotracker staining with increased concentrations of glucose. Relative protein levels of total proteins were standardized to the expression of β-Actin. All the data were shown as mean ± standard deviation. $^{*}P < 0.05$, $^{**}P < 0.01$, and $^{***}P < 0.001$.

Investigative Ophthalmology & Visual Science

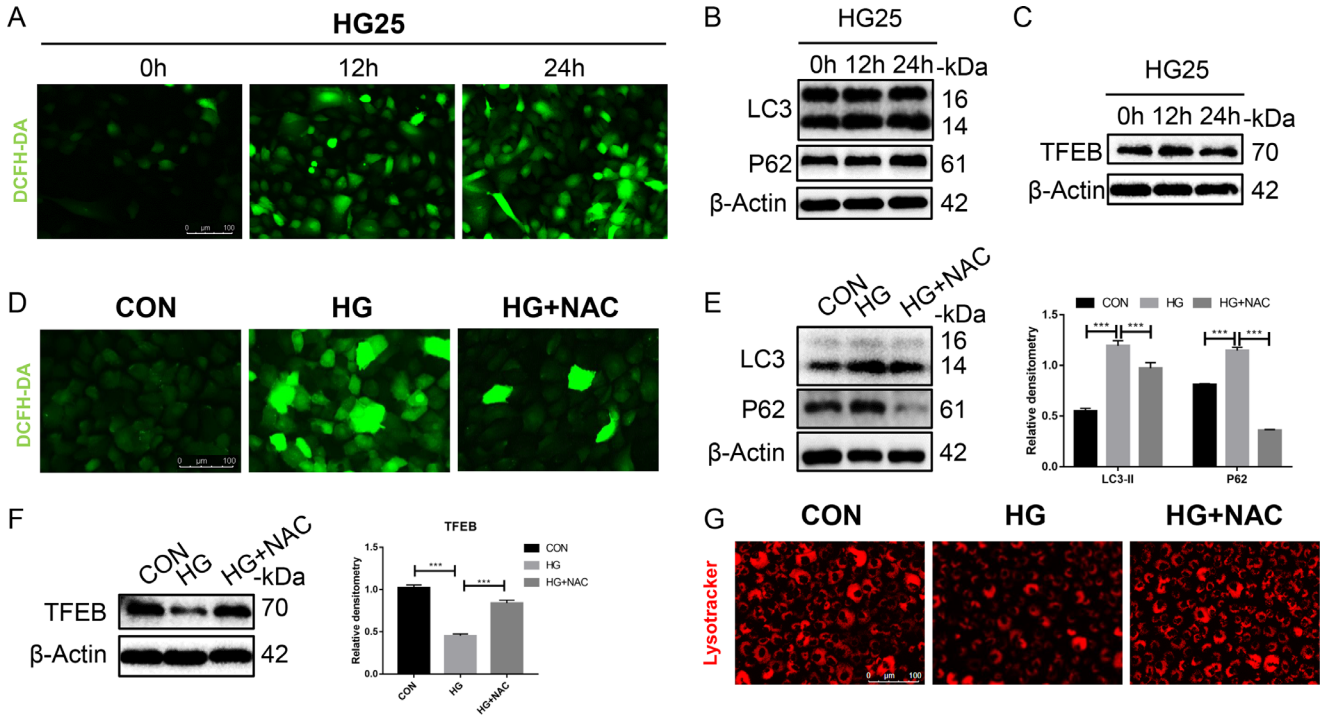

Figure 5. HG contributed to TFEB-mediated lysosomal dysfunction in a ROS-dependent manner. Primary rabbit LECs were exposed to HG (25 mM) medium. (**A**) DCFH-DA assay and (**B**) Western blot analysis showed the effects of HG treatment on ROS production and the expression levels of LC3-I/II, P62, and TFEB in LECs at 0 hours, 12 hours, and 24 hours. Next, LECs were pretreated with NAC (5 mM, 8 hours) before HG (25 mM, 3 days) administration to prevented the production of ROS. (**C**) DCFH-DA assay compared ROS levels in the control, HG, and HG + NAC groups. (**D, E**) Protein expression levels and quantitative analysis of LC3-I/II, P62, and TFEB determined by Western blotting in control, HG, and HG + NAC groups. (**F**) Lysotracker staining in the control, HG, and HG + NAC groups. All the data were shown as mean ± standard deviation. $^{*}P < 0.05$, $^{**}P < 0.01$, and $^{***}P < 0.001$.

formatic data confirmed that diabetes severely affected the development and structural integrity of the lens, highlighting the critical role of the lysosome pathway in the occurrence of DC.

HG-Induced Autophagy Blockage Resulted From TFEB-Mediated Lysosomal Dysfunction in LECs

To further explore the mechanisms of autophagy blockage, primary LECs were subjected to basal medium containing different concentrations of glucose. In agreement with previous research,[30] HG promoted EMT in LECs by raising the expression of α-SMA and FN (Fig. 4A). Subsequently, we focused on autophagy and lysosome biogenesis alterations in LECs exposed to HG. First, there was a significant increase in LC3-II and P62 in the HG groups than in the control group (Fig. 4B). Inhibition of mTOR kinase complex is a key signal for autophagosome biogenesis.[31] ATG5 and ATG7 are considered to be important molecules in inducing autophagy.[32] No differences were seen in the expression of p-mTOR, ATG5, and ATG7 (Fig. 4C), which partly ruled out that increased LC3-II resulted from over-activation of autophagy. Moreover, quantification of mCherry-EGFP-LC3 puncta indicated that HG increased autophagosomes but reduced autolysosomes in LECs (Fig. 4D), confirming a loss of autophagosome-lysosome fusion. Given the indispensable role of autophagy in delivering ubiquitinated proteins to the lysosome for clearance,[33] ubiquitin was remarkably aggregated in HG-cultured LECs (Fig. 4E). The above results confirmed that LECs were unable to degrade abnormal aggregates due to autophagy-lysosomal dysfunction after HG administration.

To investigate the role and function of lysosomes in DC, we detected the expression of the master transcription factor for lysosome (TFEB) and its antagonistic transcription factor ZKSCAN3 under HG conditions. As expected, TFEB was downregulated in HG-cultured LECs, contrary to the trend of ZKSCAN3 (see Fig. 4E). In addition, we also examined the expression of the downstream targets of TFEB, such as CTSB, a lysosomal cysteine protease and LAMP1, a component of lysosomal membrane proteins. Western blot results showed that HG inhibited the expression of CTSB compared with the control group. Instead, the expression of LAMP1 was increased in HG-cultured LECs (see Fig. 4E), but LAMP1-labeled lysosomes were larger in diameter (Fig. 4F), which also could be found in mCherry-LC3-EGFP-LC3 puncta. We speculated that the increase of LAMP1 was a feedback mechanism that strengthened LECs against HG-induced stress.[34] Indeed, the aggregation of undigested substrates was responsible for enlarged lysosomes.[35] Lysosome enlargement was considered an imbalance between lysosome fusion and fission, displaying decreased motility and secretion defect.[36–38] In addition, reduced lysotracker staining with increased HG suggested HG impaired acidic pH of lysosomal vacuoles in a concentration-dependent manner (Fig. 4G). Taken together, these results suggested that short-term HG treatment in LECs does not affect the initiation of autophagy by regulating the mTOR pathway, but inhibited the activity of the lysosomal pathway by inhibiting

Investigative Ophthalmology & Visual Science

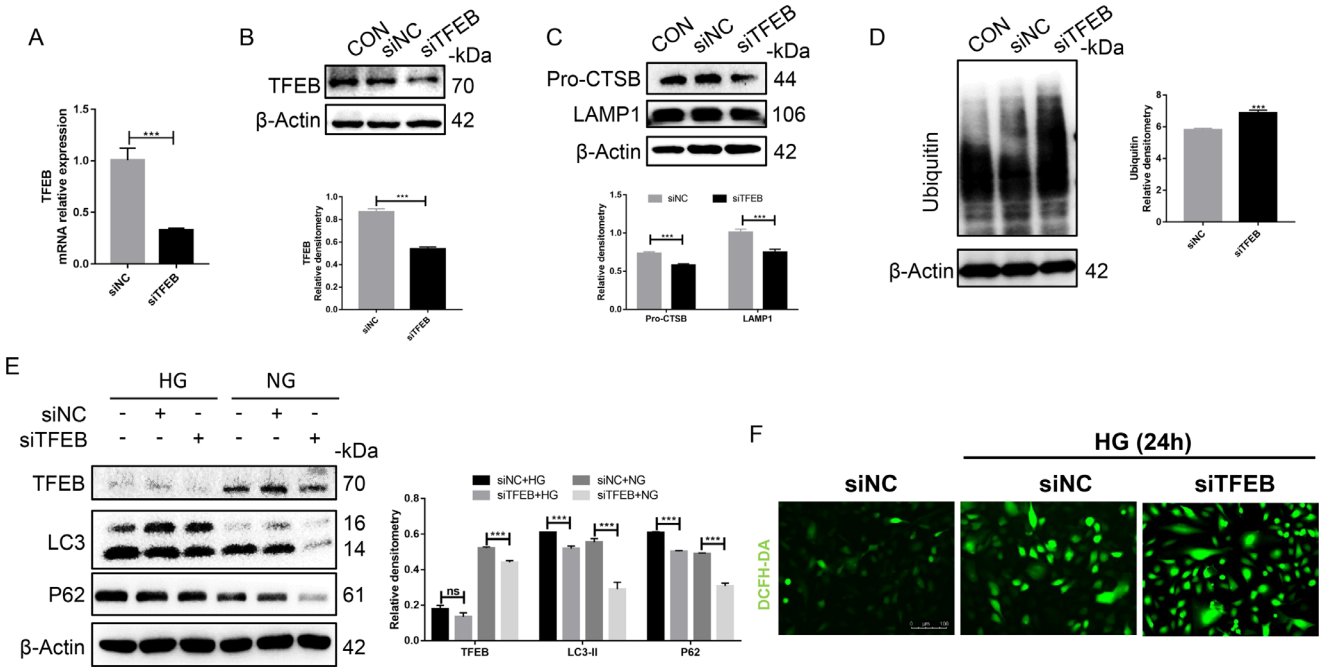

Figure 6. TFEB knockdown inhibits the autophagy-lysosomal pathway in LECs. Primary LECs were transfected with siRNAs or plasmids to knock down TFEB (Forward: 5′-CAGAAGAAAGACAAUCACATT-3′ and reverse 5′-UGUGAUUGUCUUUCUUCUGTT-3′). The expression status of TFEB was examined by (**A**) qRT-PCR and (**B**) Western blot analysis. (**C, D**) Protein expression levels and quantitative analysis of LAMP1, Pro-CTSB, and ubiquitin determined by Western blotting in LECs. (**E**) TFEB knockdown LECs were cultured under NG and HG conditions for 3 days. Western blot analysis presented the changes of LC3-I/II and P62. (**F**) DCFH-DA assay compared ROS levels in the siNC, siNC + HG, and siTFEB + HG groups. Relative protein levels of total proteins were standardized to the expression of β-Actin. The mRNA expression levels were normalized to rabbit GAPDH. All the data were shown as mean ± standard deviation. $^{*}P < 0.05$, $^{**}P < 0.01$, and $^{***}P < 0.001$.

TFEB and its downstream targets, leading to the block of autophagy.

HG Contributed to TFEB-Mediated Lysosomal Dysfunction in a ROS-Dependent Manner

It has been shown that ROS-induced lysosomal dysfunction disrupts autophagic flux in macrophages under hyperglycemic conditions.[39] To assess whether TFEB-mediated lysosomal dysfunction results from ROS accumulation in LECs, we first explored changes in ROS and autophagy and lysosomal markers upon HG treatment over time. ROS were rapidly generated after 12-hour HG treatment and continuously increased after 24-hour HG treatment (Fig. 5A), although there were no obvious changes in the expression levels of LC3-II, P62, and TFEB during 24-hour HG treatment (Figs. 5B, 5C). Thus, HG-induced ROS production preceded the initiation of HG-induced lysosomal dysfunction and autophagy blockage in LECs. Next, NAC, a commonly used membrane-permeable antioxidant compound,[40] was used to prove whether the decline of TFEB upon HG treatment resulted from excessive ROS production. The increased cellular ROS levels in LECs under HG conditions were effectively abolished by pretreatment of NAC, as shown in Figure 5D. Additionally, pretreatment of NAC significantly blocked aggregation of P62 and decrease of TFEB expression and lysosomal activities in LECs under HG conditions (Figs. 5E–G). These results indicated that HG-induced excessive generation of ROS might be a main cause of TFEB-mediated lysosomal dysfunction and autophagy blockage in LECs.

TFEB Knockdown Inhibits the Autophagy-Lysosomal Pathway in LECs

To confirm the regulatory roles of TFEB on autophagy and lysosomal biogenesis in LECs, we then inhibited TFEB expression by siRNA transient transfection. Both qPCR and Western blot analyses confirmed efficient knockdown of TFEB (Figs. 6A, 6B). As anticipated, transfection of TFEB siRNA in LECs downregulated the expression of CTSB and LAMP1 (Fig. 6C), accompanied by a remarkable ubiquitin accumulation (Fig. 6D), confirming suppressed autophagic flux. Under either NG or HG conditions, TFEB knockdown diminished the protein levels of LC3-II and P62 (Fig. 6E). Inconsistent with other studies, siTFEB transfection usually exacerbated P62 accumulation in various cells during exposure to different stimuli.[41,42] Here, we thought that genetic deletion of TFEB directly suppressed the expression of P62 in LECs, far exceeding excessive aggregation due to impaired cellular clearance. Furtherly, siTFEB aggravated HG-induced ROS generation in LECs (Fig. 6F). On the contrary, TFEB overexpression enhanced autophagic flux by inducing LC3-II upregulation and P62 downregulation (Supplementary Fig. S3). Overall, these data indicated that gene silencing of TFEB exacerbated autophagy blockade and oxidative stress by inhibiting the expression of autophagy-lysosomal genes.

TFEB Activation by C1 Exerted Suppressive Effects on HG-Induced Cataracts

As HG damaged TFEB-mediated lysosome biogenesis in LECs, we postulated that restoring the lysosomal function

Investigative Ophthalmology & Visual Science

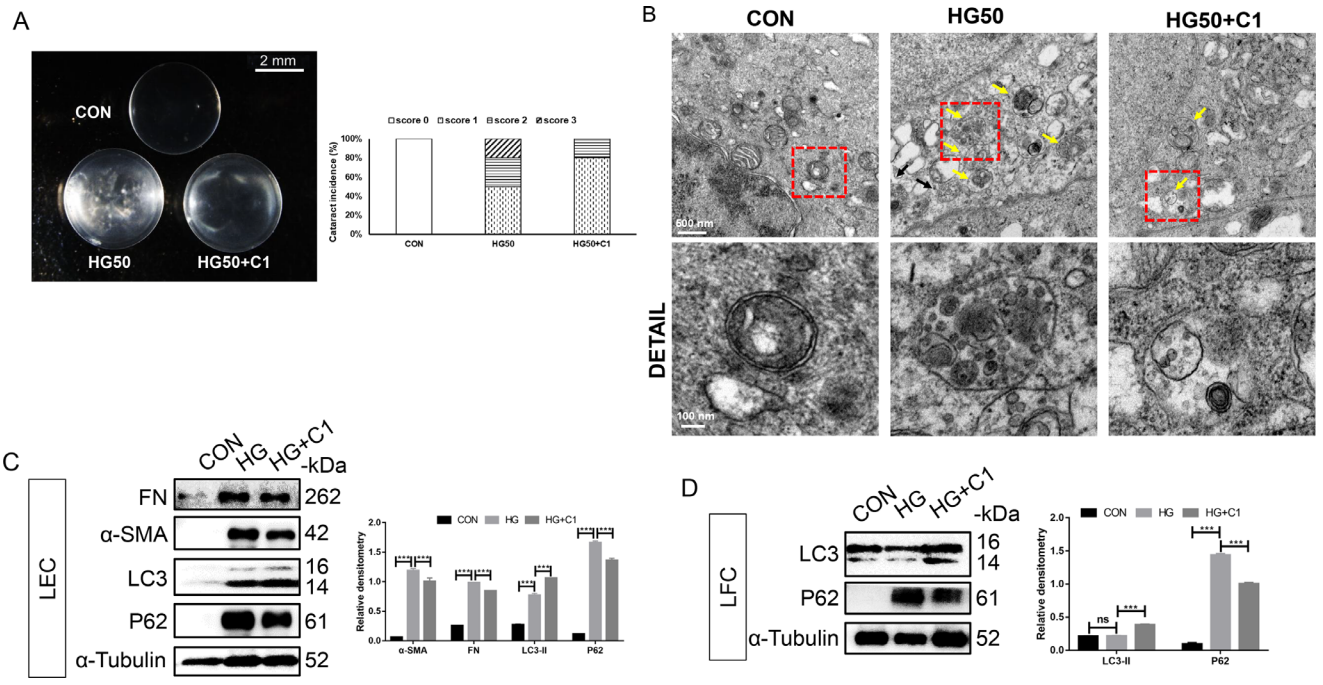

Figure 7. Curcumin analog C1 exerted protective effects in HG-induced cataracts. Rat lenses were subjected to control (5.5 mM), HG (50 mM), and HG (50 mM) with C1 (5 μM) medium for 7 days. (**A**) Representative images of cultured rat lenses and the percentage distribution of cataract scores in the control, HG, and HG + C1 groups. (**B**) TEM showed that C1 treatment alleviated abnormally large autophagic vesicles (*arrows*) with massive undegraded substrates in anterior capsular LECs under HG conditions. (**C**) Protein expression levels and quantitative analysis of α-SMA, FN, LC3-I/II, and P62 determined by Western blotting in LECs. (**D**) Protein expression levels and quantitative analysis of LC3-I/II and P62 determined by Western blotting in LFCs. All the data were shown as mean ± standard deviation. $^{*}P < 0.05$, $^{**}P < 0.01$, and $^{***}P < 0.001$.

could mitigate the injuries of HG to the lens. Lysosomal activity was then enhanced by TFEB activation via C1, an analog of curcumin. With treatment of C1 to lenses under HG conditions, lens cloudiness caused by HG was ameliorated significantly, and the corresponding cataracts were downgraded (Fig. 7A). TEM displayed that C1 treatment dramatically reduced the number of autophagic vacuoles with massive undegraded cargo in LECs from HG-cultured lenses (Fig. 7B). Further analysis showed that C1 significantly inhibited HG-induced fibrosis in LECs (Fig. 7C). Besides, incubation of HG along with C1 elevated LC3-II and declined P62 in both LECs and LFCs compared with the HG group, demonstrating that C1 reversed block in autophagy upon HG treatment (see Figs. 7C, 7D). Moreover, we also validated the effects of C1 in HG-cultured lenses of mice with low AR activity.[43] As shown in Supplementary Figure S4A, HG-cultured mouse lenses appeared cloudy for 14 days. C1 significantly diminished HG-induced EMT in LECs and increased the autophagic flux in LECs and LFCs, which was consistent with the results of rats (see Supplementary Fig. S4B, S4C).

Then, C1 was added into primary LECs cultured in HG medium to gain more insights into its protective effects. The DCFH-DA assay showed that ROS production promoted by HG was mitigated by C1 administration and TFEB activation (Fig. 8A). Consistent with the results of whole lens culture, C1 attenuated HG-induced EMT, promoted autophagic degradation, and reduced the number of large autophagic vacuoles in LECs (Figs. 8B, 8C; Supplementary Fig. S5). Furthermore, quantification of the mCherry-EGFP-LC3 puncta showed that the number of autolysosomes in the HG + C1 group was significantly higher than that in the HG groups (Fig. 8D). To identify the effect of C1 on TFEB in LECs, we compared the protein levels of the cytosolic and nuclear TFEB. HG-treated LECs exhibited downregulated TFEB expression in both nucleus and cytoplasm, whereas C1 enhanced intracellular nuclear translocation of TFEB prominently and promoted cytoplasmic TFEB expression slightly (Figs. 8E, 8F). Moreover, cotreatment of C1 and HG augmented the expression of CTSB, and LAMP1 compared with the HG group (Fig. 8G). Concomitantly, C1 incubation facilitated maintaining lysosomal acidic pH in LECs exposed to HG (Fig. 8H). In addition, it reduced the size of HG-triggered enlarged LAMP1-stained lysosomes, as well as mCherry-LC3 and EGFP-LC3 dots, indicating that C1 maintained lysosomal homeostasis (see Figs. 8D, 8H). Taken together, these results suggested that C1 activated autophagy and lysosomal biogenesis in a TFEB-dependent manner under HG treatment, thereby alleviating HG-induced cellular damage in the lens.

Comparison of THC and C1 in Alleviating HG-Induced Cataracts

As curcumin is not only an antioxidant but also an aldose reductase inhibitor,[44] it is necessary to highlight the specificity of TFEB activation in alleviating HG-induced cataracts. THC, a major bioactive metabolite of curcumin, was utilized to validate the specificity of C1 on lysosome function regulation.[45] First, we compared the effects of THC and C1 on the expression of TFEB in primary LECs. C1 restored TFEB expression under HG conditions, whereas THC had only a minor effect in elevating TFEB expression (Fig. 9A). We

Investigative Ophthalmology & Visual Science

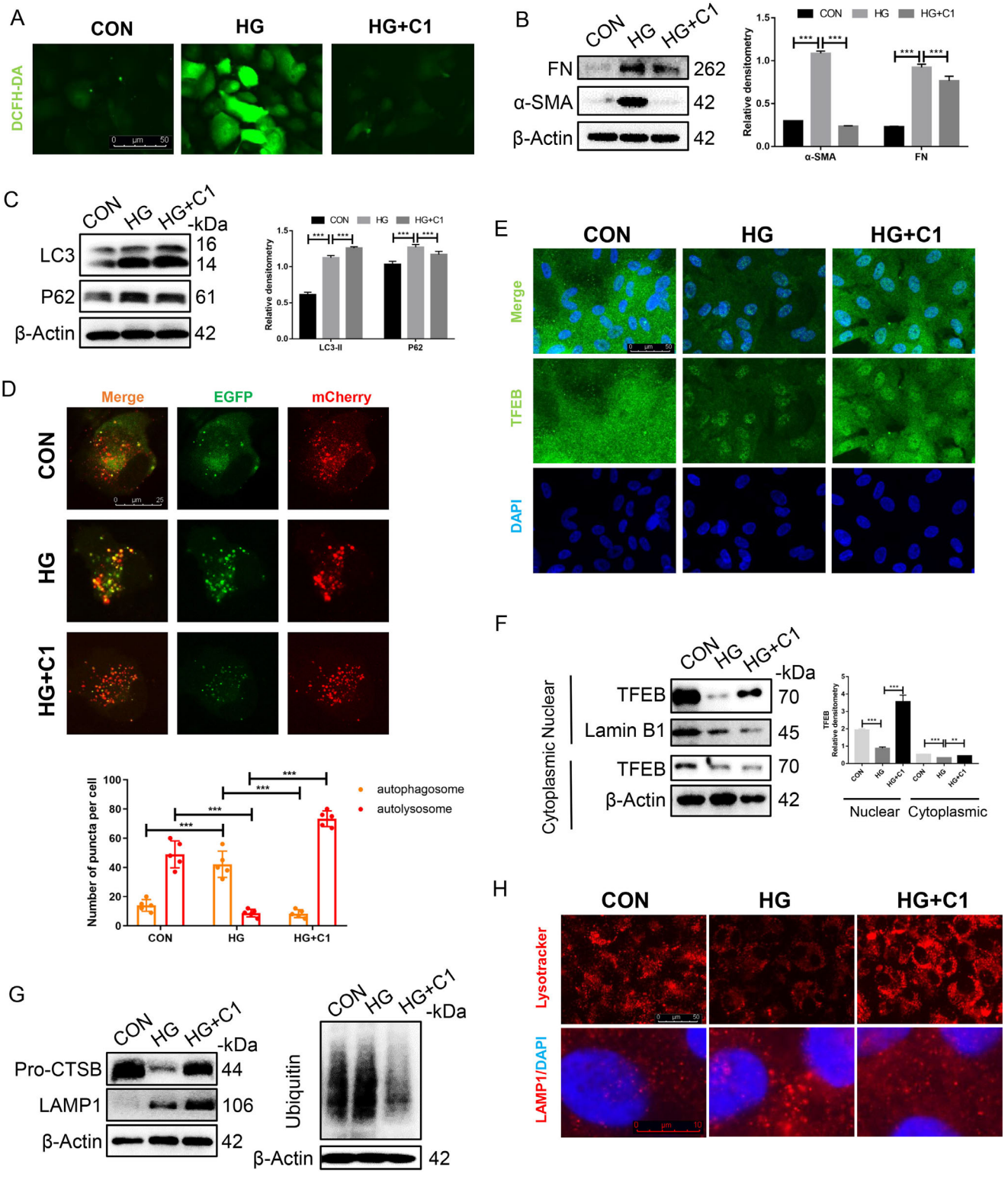

Figure 8. C1 enhanced lysosomal degradation via promoting the nuclear translocation of TFEB in HG-cultured LECs. Primary rabbit LECs were exposed to control (5.5 mM), HG (25 mM), and HG (25 mM) with C1 (5 μM) medium for 3 days. (**A**) ROS levels were detected by DCFH-DA assay. (**B, C**) Protein expression levels and quantitative analysis of α-SMA, FN, LC3-I/II, and P62 determined by Western blotting in LECs. (**D**) Representative fluorescence images of mCherry-EGFP-LC3 puncta within LECs and quantification. (**E**) Immunofluorescence staining and Western blot analysis (**F**) showed that C1 increased the expression levels and distributions of TFEB in the cytoplasm and nuclei in LECs. (**G**) Protein expression levels and quantitative analysis of Pro-CTSB, LAMP1, and ubiquitin determined by Western blotting in LECs. (**H**) Lysotracker staining and immunofluorescence staining of LAMP1 puncta in LECs. Relative protein levels of total proteins were standardized to the expression of β-Actin, whereas nuclear proteins were normalized to Lamin B1. All the data were shown as mean ± standard deviation. $^{*}P < 0.05$, $^{**}P < 0.01$, and $^{***}P < 0.001$.

Investigative Ophthalmology & Visual Science

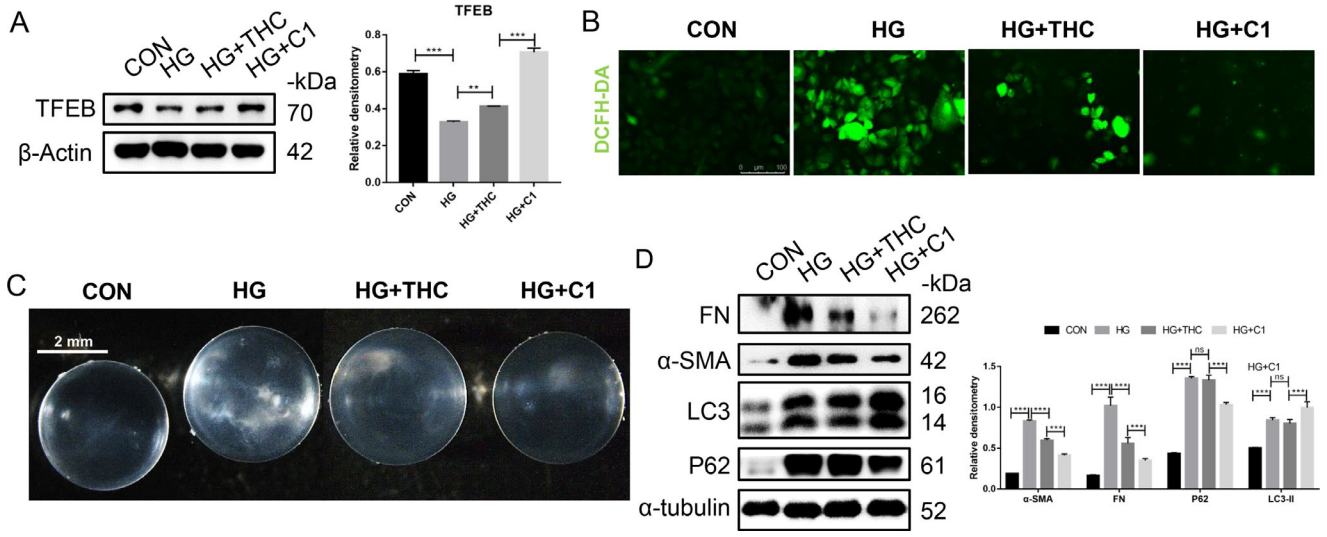

Figure 9. Comparison of THC and C1 in alleviating HG-induced cataracts. Primary rabbit LECs were exposed to control (5.5 mM), HG (25 mM), HG (25 mM) with THC (5 μM), and HG (25 mM) with C1 (5 μM) medium for 3 days. (**A**) Protein expression levels and quantitative analysis of TFEB determined by Western blotting in LECs. (**B**) DCFH-DA assay compared ROS levels in the control, HG, HG + THC, and HG + C1 groups. Rat lenses were subjected to control (5.5 mM), HG (50 mM), HG (50 mM) with THC (5 μM), and HG (50 mM) with C1 (5 μM) medium for 7 days. (**C**) Representative images of cultured rat lenses and the percentage distribution of cataract scores in the control, HG, HG + THC, and HG + C1 groups. (**D**) Protein expression levels and quantitative analysis of α-SMA, FN, LC3-I/II, and P62 determined by Western blotting in LECs. All the data were shown as mean ± standard deviation. $^{*}P < 0.05$, $^{**}P < 0.01$, and $^{***}P < 0.001$.

further compared the antioxidant activities between C1 and THC upon HG administration. As shown in Figure 9B, C1 had a much stronger effect against HG-induced ROS than THC. Next, we compared the protective effects of THC and C1 in HG-cultured lenses. As shown in Figure 9C, compared to THC, C1 displayed a more pronounced effect in alleviating lens cloudiness induced by HG than THC. Further molecular analysis showed that C1 had more potent effects in reversing HG-induced EMT and autophagy blockage than THC (Fig. 9D). Therefore, we considered that TFEB activation could promote autophagic flux to enhance antioxidant capacity, which may explain this discrepancy between C1 and THC in attenuating HG-induced cataracts.

Discussion

Among the pathogenic mechanisms of DC, previous studies demonstrate that HG-induced AR overactivation and excessive ROS production are the main triggers for lenticular injuries progression.[46] However, the exact mechanisms of how HG undermines the lens cells or how the lens cells respond to HG-related stress remain largely unexplored. Apart from the glycation and oxidation stress, autophagy-lysosomal dysfunction was identified to be a deeper molecular mechanism in the development of DC for the first time in this study, and the defect of lysosomal degradation was revealed as a critical factor in rupture of lens cells and lens opacification during the formation of diabetic cataract.

In both DM rats as well as HG-cultured lens tissue and cell models, we observed that HG promoted EMT of LECs, which further caused swelling, disordered arrangement, and abnormal denucleation of LFCs, thus resulting in lens opacity. Meanwhile, RNA-seq data and TEM analysis showed vesicle retention and substrates accumulation in lens cells due to inhibition of lysosome synthesis and degradation upon HG stimulation. Protein analyses and immunostaining of tissues and cells also presented that EMT was accompanied by increased P62 in LECs, suggesting abnormal autophagy degradation under HG conditions. Therefore, these results indicated that homeostatic disruption of lens cells might be correlated with the impairment of lysosomal function.

To confirm the influence of lysosomal function on lens cells upon HG exposure, we further investigated transcription factors critical for lysosomal biogenesis in LECs under HG conditions. TFEB is a master gene for lysosomal biogenesis that coordinated this program by driving the expression of autophagy and lysosomal genes, whereas ZKSCAN3 has the opposite effect.[47] In our study, HG upregulated the expression of ZKSCAN3, whereas downregulated TFEB expression and suppressed its nuclear translocation in LECs. Our results further indicated that ROS overload caused impaired autophagosome clearance by disrupting TFEB-mediated lysosomal function under the diabetic condition. TFEB knockdown inhibited the autophagic flux, which was evidenced by the decreased expression of the lysosomal enzyme (CTSB), lysosomal-associated membrane protein (LAMP1) and enhanced ubiquitin accumulation in LECs under HG conditions. In contrast, overexpression of TFEB enhanced autophagy flux in HG-treated LECs. Furthermore, TFEB activation by curcumin analog C1 increased lysosomal function, promoted autophagic flux and eliminated oxidizing molecules, thus restoring epithelial properties of LECs and lens transparency under HG conditions. A previous study has reported that curcumin itself can retard the progression of STZ-induced DC in rats by suppressing oxidative stress and AR activity.[48] Compared with a metabolite of curcumin (THC), C1 was more effective in alleviating lens opacity caused by HG through attenuating HG-induced autophagy blockage and ROS production. Additionally, C1 exerted protective effects in HG-induced lens cloudiness in mouse lenses with low AR activity by promoting lysosomal degradation. Taken together, TFEB-mediated lysosomal function plays a crucial role in maintaining cellular homeostasis of LECs and lens transparency under HG conditions.

Investigative Ophthalmology & Visual Science

HG and oxidative stress can induce EMT and apoptosis in LECs, thus leading to cataract formation.[8,49] In the present study, we preliminarily demonstrated that ROS was an upstream event in TFEB-mediated lysosomal impairment, autophagy blockage, and subsequently a series of injury responses in the lens. In addition, downregulation of TFEB expression further exacerbated oxidative damage via aggravating autophagy blockage in LECs. TFEB activation by C1 could enhance the resistance to HG-induced oxidative stress in the lens. Previous studies have proved that ROS-TFEB-dependent lysosomal dysfunction disrupts autophagic flux in macrophages and retinal Müller cells under hyperglycemic conditions.[39,50] Moreover, TFEB-mediated lysosomal deficiency could cause a failure in degrading damaged organelles, including mitochondria, thus further aggravating ROS production.[51] ROS accumulation could give rise to a series of downstream events including canonical DNA damage, thereby stimulating the p53 pathway,[52] which was activated in DC rat lens cells according to our RNA-seq data. Accumulation of these damages might further induce cell death. Conversely, in response to oxidative stress, autophagy could clear increased cytosolic ROS and proteins damaged by ROS to reduce cell injury and promote cell survival.[53] Therefore, HG can induce oxidative damage and lysosomal defects, which might further exacerbate ROS generation, and TFEB activation can increase antioxidant resistance in the lens. Research in cross-talk of redox regulation and lysosomal function would also be very interesting and meaningful in the future.

In summary, our study for the first time revealed that HG destructed TFEB-mediated abnormal lysosomal degradation in a ROS-dependent manner, leading to autophagy blockage, and eventually impairment of lens cells and lens opacification (Supplementary Fig. S6). Hence, these findings suggest that combining lysosomal restoration with antioxidation could be applied in prevention and treatment strategies for DC. Here, we have solely proved that promoting lysosomal function by TFEB activation can effectively restore LECs function and lens transparency in vitro diabetic cataract tissue culture model, and further in vivo experiments are required to validate the efficiency and safety of lysosome function enhancement in preventing or repressing DC.

Acknowledgments

The authors thank the staff of Core Facilities at State Key Laboratory of Ophthalmology, Zhongshan Ophthalmic Center for technical support.

Supported by National Natural Science Foundation of China (No. 82070944 and No. 81721003), Guangdong Basic and Applied Basic Research Foundation (No. 2021A1515111078), the State Key Laboratory of Ophthalmology, Zhongshan Ophthalmic Center, Sun Yat-Sen University.

Disclosure: **Y. Sun**, None; **X. Wang**, None; **B. Chen**, None; **M. Huang**, None; **P. Ma**, None; **L. Xiong**, None; **J. Huang**, None; **J. Chen**, None; **S. Huang**, None; **Y. Liu**, None

References

1. Pollreisz A, Schmidt-Erfurth U. Diabetic Cataract—Pathogenesis, Epidemiology and Treatment. *J Ophthalmol.* 2010;2010:1–8.
2. Kiziltoprak H, Tekin K, Inanc M, Goker YS. Cataract in diabetes mellitus. *World J Diabetes*. 2019;10:140–153.
3. Grzybowski A, Kanclerz P, Huerva V, et al. Diabetes and Phacoemulsification Cataract Surgery: Difficulties, Risks and Potential Complications. *J Clin Med*. 2019;8:716.
4. Cvekl A, Zhang X. Signaling and Gene Regulatory Networks in Mammalian Lens Development. *Trends Genet*. 2017;33:677–702.
5. Tjahjono N, Xia CH, Li R, et al. Connexin 50-R205G Mutation Perturbs Lens Epithelial Cell Proliferation and Differentiation. *Invest Ophthalmol Vis Sci*. 2020;61:25.
6. Tang WH, Martin KA, Hwa J. Aldose Reductase, Oxidative Stress, and Diabetic Mellitus. *Front Pharmacol*. 2012;3:87.
7. Babizhayev MA, Yegorov YE. Reactive Oxygen Species and the Aging Eye: Specific Role of Metabolically Active Mitochondria in Maintaining Lens Function and in the Initiation of the Oxidation-Induced Maturity Onset Cataract–A Novel Platform of Mitochondria-Targeted Antioxidants With Broad Therapeutic Potential for Redox Regulation and Detoxification of Oxidants in Eye Diseases. *Am J Ther.* 2016;23:e98–e117.
8. Li J, Chen Y, Han C, et al. JNK1/β-catenin axis regulates H(2)O(2)-induced epithelial-to-mesenchymal transition in human lens epithelial cells. *Biochem Biophys Res Commun*. 2019;511:336–342.
9. Giacco F, Brownlee M. Oxidative stress and diabetic complications. *Circ Res*. 2010;107:1058–1070.
10. Snow A, Shieh B, Chang K, et al. Aldose reductase expression as a risk factor for cataract. *Chem Biol Interact*. 2015;234:247–253.
11. Ma Z, Liu J, Li J, et al. Klotho ameliorates the onset and progression of cataract via suppressing oxidative stress and inflammation in the lens in streptozotocin-induced diabetic rats. *Int Immunopharmacol*. 2020;85:106582.
12. Nambu H, Kubo E, Takamura Y, et al. Attenuation of aldose reductase gene suppresses high-glucose-induced apoptosis and oxidative stress in rat lens epithelial cells. *Diabetes Res Clin Pract*. 2008;82:18–24.
13. Kitada M, Koya D. Autophagy in metabolic disease and ageing. *Nat Rev Endocrinol*. 2021;17:647–661.
14. Yu L, Chen Y, Tooze SA. Autophagy pathway: Cellular and molecular mechanisms. *Autophagy*. 2017;14:207–215.
15. Yan X, Zhou R, Ma Z. Autophagy-Cell Survival and Death. *Adv Exp Med Biol*. 2019;1206:667–696.
16. Ding Y, Choi ME. Autophagy in diabetic nephropathy. *J Endocrinol*. 2015;224:R15–R30.
17. Rosa MD, Distefano G, Gagliano C, et al. Autophagy in Diabetic Retinopathy. *Curr Neuropharmacol*. 2016;14:810–825.
18. Morishita H, Mizushima N. Autophagy in the lens. *Exp Eye Res*. 2016;144:22–28.
19. Chen J, Ma Z, Jiao X, et al. Mutations in FYCO1 Cause Autosomal-Recessive Congenital Cataracts. *Am J Hum Genet*. 2011;88:827–838.
20. Mrakovic A, Kay JG, Furuya W, et al. Rab7 and Arl8 GTPases are necessary for lysosome tubulation in macrophages. *Traffic*. 2012;13:1667–1679.
21. Morishita H, Eguchi S, Kimura H, et al. Deletion of autophagy-related 5 (Atg5) and Pik3c3 genes in the lens causes cataract independent of programmed organelle degradation. *J Biol Chem*. 2013;288:11436–11447.
22. Li J, Ye W, Xu W, et al. Activation of autophagy inhibits epithelial to mesenchymal transition process of human lens epithelial cells induced by high glucose conditions. *Cell Signal*. 2020;75:109768.
23. Kametaka S, Kasahara T, Ueo M, et al. A Novel High Resolution In Vivo Digital Imaging System for the Evaluation

of Experimental Cataract in Diabetic Rats. *J Pharmacol Sci*. 2008;106:144–151.
24. Hales AM, Chamberlain CG, McAvoy JW. Susceptibility to TGFbeta2-induced cataract increases with aging in the rat. *Invest Ophthalmol Vis Sci*. 2000;41:3544–3551.
25. Lin H, Ouyang H, Zhu J, et al. Lens regeneration using endogenous stem cells with gain of visual function. *Nature*. 2016;531:323–328.
26. Chaffee BR, Shang F, Chang ML, et al. Nuclear removal during terminal lens fiber cell differentiation requires CDK1 activity: appropriating mitosis-related nuclear disassembly. *Development*. 2014;141:3388–3398.
27. Lück C, Haitjema C, Heger C. Simple Western: Bringing the Western Blot into the Twenty-First Century. *Methods Mol Biol*. 2021;2261:481–488.
28. Saftig P, Haas A. Turn up the lysosome. *Nat Cell Biol*. 2016;18:1025–1027.
29. Nakahara M, Nagasaka A, Koike M, et al. Degradation of nuclear DNA by DNase II-like acid DNase in cortical fiber cells of mouse eye lens. *The FEBS Journal*. 2007;274:3055–3064.
30. Du L, Hao M, Li C, et al. Quercetin inhibited epithelial mesenchymal transition in diabetic rats, high-glucose-cultured lens, and SRA01/04 cells through transforming growth factor-β2/phosphoinositide 3-kinase/Akt pathway. *Mol Cell Endocrinol*. 2017;452:44–56.
31. Munson MJ, Ganley IG. MTOR, PIK3C3, and autophagy: Signaling the beginning from the end. *Autophagy*. 2015;11:2375–2376.
32. Arakawa S, Honda S, Yamaguchi H, Shimizu S. Molecular mechanisms and physiological roles of Atg5/Atg7-independent alternative autophagy. *Proc Jpn Acad Ser B Phys Biol Sci*. 2017;93:378–385.
33. Rogov V, Dötsch V, Johansen T, Kirkin V. Interactions between autophagy receptors and ubiquitin-like proteins form the molecular basis for selective autophagy. *Mol Cell*. 2014;53:167–178.
34. Tseng HHL, Vong CT, Kwan YW, et al. Lysosomal Ca2+ Signaling Regulates High Glucose-Mediated Interleukin-1β Secretion via Transcription Factor EB in Human Monocytic Cells. *Front Immunol*. 2017;8:1161.
35. Scerra G, De Pasquale V, Pavone LM, et al. Early onset effects of single substrate accumulation recapitulate major features of LSD in patient-derived lysosomes. *iScience*. 2021;24:102707.
36. Choy CH, Saffi G, Gray MA, et al. Lysosome enlargement during inhibition of the lipid kinase PIKfyve proceeds through lysosome coalescence. *J Cell Sci*. 2018;131:jcs213587.
37. Durchfort N, Verhoef S, Vaughn MB, et al. The Enlarged Lysosomes in beigej Cells Result From Decreased Lysosome Fission and Not Increased Lysosome Fusion. *Traffic*. 2012;13:108–119.
38. Devi TS, Yumnamcha T, Yao F, et al. TXNIP mediates high glucose-induced mitophagic flux and lysosome enlargement in human retinal pigment epithelial cells. *Biol Open*. 2019;8:bio038521.
39. Yuan Y, Chen Y, Peng T, et al. Mitochondrial ROS-induced lysosomal dysfunction impairs autophagic flux and contributes to M1 macrophage polarization in a diabetic condition. *Clin Sci (Lond)*. 2019;133:1759–1777.
40. Tenório M, Graciliano NG, Moura FA, et al. N-Acetylcysteine (NAC): Impacts on Human Health. *Antioxidants (Basel)*. 2021;10:967.
41. Wu Y, Xun Y, Zhang J, et al. Resveratrol Attenuates Oxalate-Induced Renal Oxidative Injury and Calcium Oxalate Crystal Deposition by Regulating TFEB-Induced Autophagy Pathway. *Front Cell Dev Biol*. 2021;9:638759.
42. Sun X, Chang R, Tang Y, et al. Transcription factor EB (TFEB)-mediated autophagy protects bovine mammary epithelial cells against H2O2-induced oxidative damage in vitro. *J Anim Sci Biotechnol*. 2021;12:35.
43. Wen Y, Bekhor I. Levels of expression of hexokinase, aldose reductase and sorbitol dehydrogenase genes in lens of mouse and rat. *Curr Eye Res*. 1993;12:323–332.
44. Katsori AM, Chatzopoulou M, Dimas K, et al. Curcumin analogues as possible anti-proliferative & anti-inflammatory agents. *Eur J Med Chem*. 2011;46:2722–2735.
45. Li K, Zhai M, Jiang L, et al. Tetrahydrocurcumin Ameliorates Diabetic Cardiomyopathy by Attenuating High Glucose-Induced Oxidative Stress and Fibrosis via Activating the SIRT1 Pathway. *Oxid Med Cel Longev*. 2019;2019:6746907.
46. Greenberg MJ, Bamba S. Diabetic cataracts. *Dis Mon*. 2021:101134.
47. Medina DL, Fraldi A, Bouche V, et al. Transcriptional Activation of Lysosomal Exocytosis Promotes Cellular Clearance. *Dev Cell*. 2011;21:421–430.
48. Suryanarayana P, Saraswat M, Mrudula T, et al. Curcumin and Turmeric Delay Streptozotocin-Induced Diabetic Cataract in Rats. *Invest Ophthalmol Vis Sci*. 2005;46:2092.
49. Han ZH, Wang F, Wang FL, et al. Regulation of transforming growth factor β-mediated epithelial-mesenchymal transition of lens epithelial cells by c-Src kinase under high glucose conditions. *Exp Ther Med*. 2018;16:1520–1528.
50. Singh LP, Devi TS. Potential Combination Drug Therapy to Prevent Redox Stress and Mitophagy Dysregulation in Retinal Müller Cells under High Glucose Conditions: Implications for Diabetic Retinopathy. *Diseases*. 2021;9:91.
51. Zhang Z, Yan J, Bowman AB, et al. Dysregulation of TFEB contributes to manganese-induced autophagic failure and mitochondrial dysfunction in astrocytes. *Autophagy*. 2020;16:1506–1523.
52. Gong L, Liu F, Xiong Z, et al. Heterochromatin protects retinal pigment epithelium cells from oxidative damage by silencing p53 target genes. *Proc Natl Acad Sci USA*. 2018;115:E3987–E3995.
53. Filomeni G, De Zio D, Cecconi F. Oxidative stress and autophagy: the clash between damage and metabolic needs. *Cell Death Differ*. 2015;22:377–388.

Investigative Ophthalmology & Visual Science